V. KLEMAS
W. D. PHILPOT
University of Delaware
Newark, DE 19711

Drift and Dispersion Studies of Ocean-Dumped Waste Using Landsat Imagery and Current Drogues

The magnitudes of plume drift velocities, determined from Landsat imagery, were compatible with the drift velocities of current drogues released over a 12-month period.

ABSTRACT: *The drift and dispersion of industrial acid wastes dumped 64 km off the Delaware coast was investigated. Waste plume drift velocities and spread rates were obtained from 16 Landsat images, which were analyzed by optical and digital techniques. Principal component (eigenvector) analysis was performed to discriminate the acid waste from other pollutants and minimize cloud cover effects. Most of the 16 waste plumes imaged by Landsat were found to be drifting at average rates of 0.59 km hr^{-1} (0.28 knot) to 3.39 km hr^{-1} (1.83 knots) into the southwest quadrant. The plumes seemed to remain above the thermocline, which was observed to form from June through August at depths ranging from 13 m to 24 m. The magnitudes of plume drift velocities were compatible with the drift velocities of current drogues released over a 12-month period. Rapid waste movement toward shore occurred primarily during storms, particularly northeasters. During such storms, however, the plume was rapidly dispersed and diluted. Landsat data analysis indicates that the plume width increased at a rate of about 1.5 cm sec^{-1} during calm sea conditions and attained average spread rates of 4 cm sec^{-1} on days when winds reached speeds of 25 km hr^{-1} (13 knots) to 38 km hr^{-1} (21 knots).*

INTRODUCTION

FEW SCIENTISTS agree on the magnitude of the environmental threat posed to coastal living resources by ocean dumping and waste disposal on the continental shelf. However, there is agreement on the need for monitoring the dispersion and effects of the wastes being dumped. As the dump sites are moved further from shore, ship surveys become excessively expensive. Therefore, remote sensing techniques, including satellites, aircraft, and buoys or drogues become attractive for this task. Remote sensors do not eliminate the need for ship observations but rather supplement ship measurements by minimizing expensive ship time and extending synoptic observations to larger coastal regions. The purpose of this paper is to present results of Landsat and current drogue studies of the drift and dispersion of industrial wastes dumped at a site 64 km off the coast of Delaware.

WASTE COMPOSITION AND DISPOSAL

The barged wastes come from the manufacture of titanium dioxide pigment. The specially designed barge, described by Fader (1972), is 82 m long, 18 m wide, and 5.5 m deep, and has a total capacity of about 3800 m^3 (1 million gallons).

PHOTOGRAMMETRIC ENGINEERING AND REMOTE SENSING,
Vol. 47, No. 4, April 1981, pp. 533-542.

Radio-controlled signals from a towing tug release the waste from the unmanned barge in a designated disposal area.

Wastes flow from the barge by gravity at a controlled rate into a disposal area recommended by the U.S. Interior Department's Bureau of Commercial Fisheries (now the National Marine Fisheries Service, Department of Commerce). The waste disposal area encompasses a rectangle of 9.3 km by 14.8 km centered approximately 73 km southeast of Cape Henlopen, Delaware. The area is bounded by 38°30′ and 38°35′ north latitude, and 74°15′ and 74°25′ west longitude. The sea throughout the area is between 38 m and 48 m deep. The barge is towed to sea approximately two to three times a week. Initially the discharge time was about 1 hour at a speed of 11 km hr^{-1} (6 knots), weather and other conditions permitting. Since May 1974 a bow tie dump pattern was adopted with a discharge time of about 5 hours at a speed of 15 km hr^{-1} (8 knots). The waste originally was 17 to 23 percent acid (expressed as H_2SO_4) and 4 to 10 percent ferrous sulfate (Falk, 1974). During 1975 the composition of the waste was changed to a solution of 10 percent acid (expressed as HCl) and 4 percent iron as iron chloride salts (EPA, 1975). Similar wastes have been disposed at sea for 30 years in the New York Bight (Peschiera *et al.*, 1968).

A limited amount of information on the waste disposal site is given by Hydrographic Office bathymetric charts and in papers by Bumpus (1965, 1969, 1973), Ketchum (1953), and Myers (1974). Their work included releases of bottom drifters and surface floats. Bumpus (1965) observed a line parallel to the shore at approximately 55 to 64 m depth where bottom drifters released inside of this line move shoreward and drifters released outside of the line move offshore. This line lies approximately 69 km off the coast of Delaware. Myers found that isothermal conditions prevailed throughout the water column during winter and spring months until mid-April, when a distinct thermocline formed between 18 and 23 m depth.

A study conducted by Falk (1974), at the time when the waste was disposed in a 1-hour period, included Eulerian type current measurements with current meters. They found that the ocean currents were southwesterly at the bottom. In the summer, the stratified surface waters moved north or northwesterly. The general movement of the waste field was to the southwest, except during late spring and summer when the wastes above the thermocline moved to the northwest.

Satellite Observations

The frequency of the dumping made it possible for Landsat satellites and aircraft to observe the waste plumes in various stages of dispersion ranging from minutes to days after dump completion. Sixteen satellite images taken from October 1972 to March 1976 were found which show water discoloration in the general vicinity of the waste dump site (Klemas *et al.*, 1977a). The spectral characteristics and position of the discoloration, the dump pattern, and the time difference between the dump and photograph gave strong indications that the discolorations are the waste plume (Figure 1).

There is considerable shearing and dispersion of the waste plume during a 3.3 hour period (Figures 1 and 2). Spectrometric measurements indicate that, upon combining with seawater, the waste develops a strong reflectance peak in the 550 to 600 nanometre region, resulting in a stronger contrast in the Landsat Band 4 than the other bands. This spectral appearance seems to be caused by the formation of a sparse but optically persistent suspended ferric floc (Ohlhorst and Bahn, 1979).

Landsat imagery was analyzed by visual and digital techniques to obtain information on acid waste plume drift, spreading (dispersion), and discrimination from other substances. Landsat images of the acid waste plumes obtained on sixteen different dates were used to photogrammetrically measure the drift distance and direction of the plumes from the recorded dump coordinates (Fig-

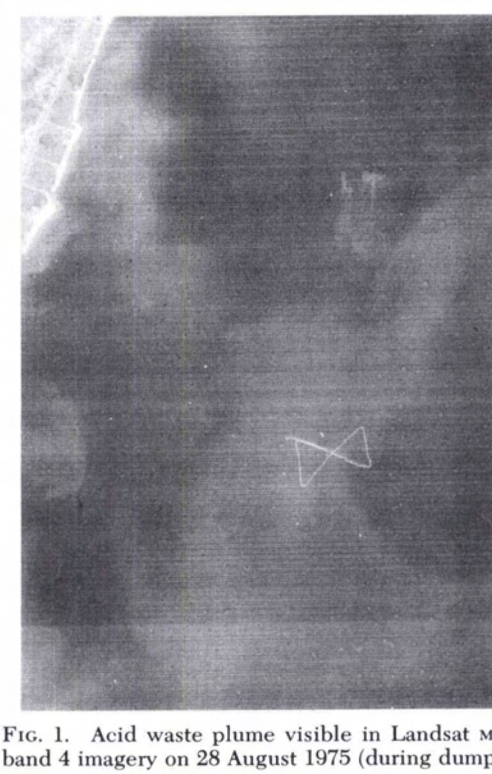

Fig. 1. Acid waste plume visible in Landsat MSS band 4 imagery on 28 August 1975 (during dump).

FIG. 2. Acid waste plume visible in Landsat MSS band 4 imagery on 24 February 1976 (3 hours and 23 minutes after dump completion).

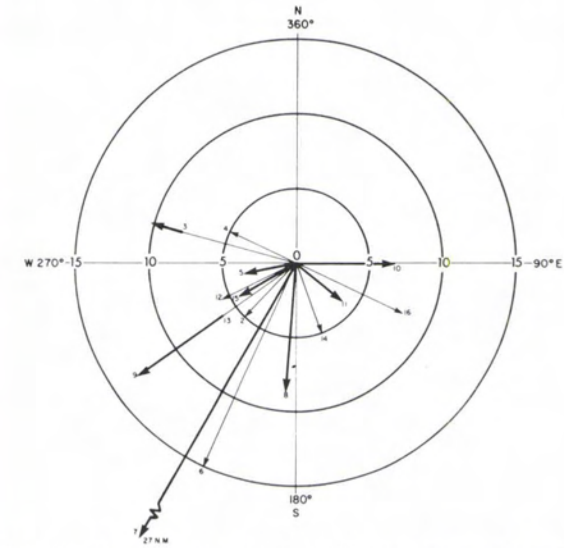

FIG. 3. Distance from center of dump site to estimated centroid of imaged plume in nautical miles.

ure 3). Drift distances and directions were measured directly from enlarged Landsat film products, some of which were optically enhanced. Plume drift speeds were calculated by dividing the distance between plume centroid and the center of the waste dump site by the time between dump and satellite overpass. The dump time was defined as the midpoint between waste dump initiation and completion. Barge captain's logs were consulted to validate this procedure. The authors' observations confirm the contention that most of the waste dumps are centered on the proper site.

Plume spread (dispersion) data, as shown in Figure 4, were obtained by performing digital analysis on Band 4 of the same sixteen Landsat overpass dates. Both digital computer print-outs and enlarged/enhanced film products were used for this analysis. Since the plume width during dumping was known from aircraft and boat measurements and the time difference between dump and overpass was also known, measurement of plume width in the Landsat images enabled us to calculate plume spreading (dispersion) rates. To

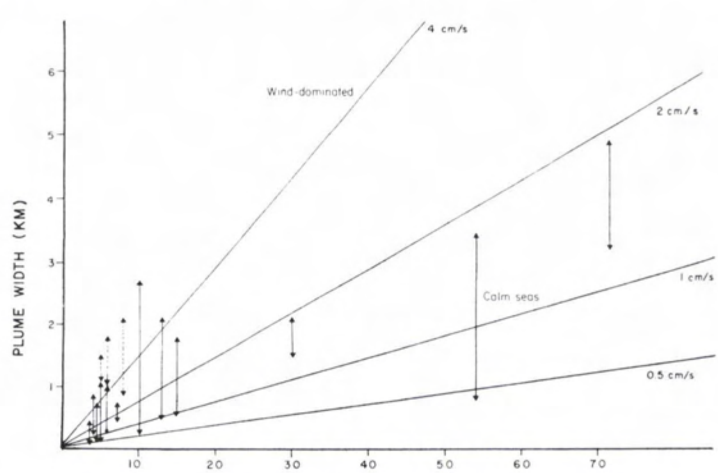

FIG. 4. Acid waste plume width as a function of time after dump.

differentiate acid waste plumes from other pollutants and clouds, principal component (eigenvector) analysis was performed using all four Landsat MSS bands.

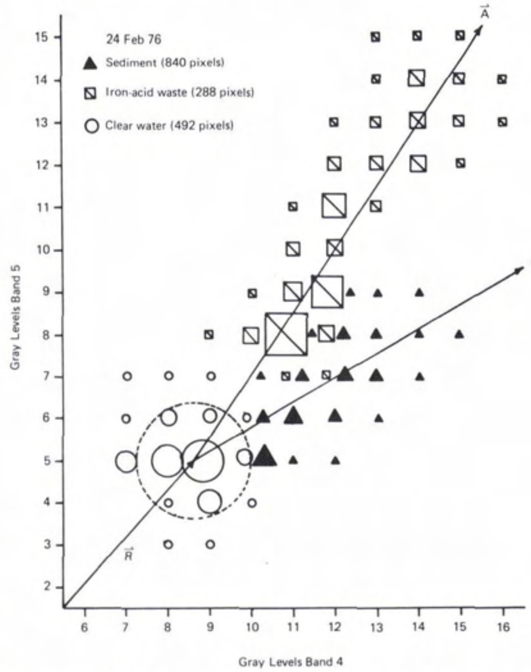

FIG. 5. Two-band gray level plot of clear water, sediment-laden water, and iron-acid waste.

MULTISPECTRAL ANALYSIS AND ENHANCEMENT OF LANDSAT IMAGERY

The use of spectral reflectance characteristics to identify substances in the water has attracted considerable attention in the past several years (Mueller, 1976; Gordon *et al.*, 1975; Hovis, 1977; Gordon, 1978; Johnson and Ohlhorst, 1980; Plass *et al.*, 1978). Our approach is most similar to that suggested by Mueller (1976)—eigenvector (principal component) analysis. Eigenvector analysis has been described by a number of investigators, including Mueller (1976) and Simmonds (1963). Perhaps the best and most complete presentation can be found in Morrison (1976); the reader is referred to this text for a detailed discussion of the technique.

One major reason for using eigenvector analysis is that it allows the reduction of significant variates with minimal loss of information. With Landsat/MSS data there are only four spectral bands and therefore only four variables to begin with, and the analysis will rarely reduce this number by more than one. However, the eigenvectors can also provide an efficient representation of variations in water color which can be readily adapted to an automatic classification process.

To illustrate the technique, we will consider Landsat data from the 24 February 1976 overpass of the Delaware-New Jersey Coast. The waters in Delaware Bay were relatively heavily sediment laden; the offshore waters were quite clear except for the presence of an iron-acid waste plume at the offshore dumpsite.

If the atmospheric conditions are constant over the scene, the spectral radiance from clear water viewed at the satellite should also be constant over the scene. The addition of any material to the water should then cause the observed spectral radiance to deviate from the ambient water signature. Initially, we assume that the change in color will be characteristic of the added material and that the color *change* will be independent of the optical characteristics of the ambient water.

A plot of the gray levels in two spectral bands of each picture element (pixel) should then resemble Figure 5 which is a Band 4 vs Band 5 plot of pixels representing clear water (circles), sediment-laden water (squares), and the iron acid waste (triangles). The size of the symbols is proportional to the number of pixels at that point.

This simplified version of ocean color can be described effectively using eigenvector analysis. The characteristic vectors are found for each substance separately using the ambient water signature as the mean, $\boldsymbol{R}$. The effect is to define vectors $\bar{\boldsymbol{A}}$ and $\bar{\boldsymbol{B}}$ in Figure 5 (corresponding to the first principal components for substance 1 and 2, respectively). Eigenvector analysis also provides measures of the dispersion of the data about the axis of the first characteristic vector. The procedure is covered in considerable detail by Klemas *et al.* (1978), including the classification procedures in the region of overlap near the clear water locus (Figure 5).

There are two comments to be made at this point. First of all, most multispectral systems have more than two bands. Thus, even if two targets are identical in two of the bands, they may be separable in other bands. Each band is considered as an added dimension in color space. Increasing the dimensions of the system increases the conceptual complexity and increases the computation time required for the decision process, but the mathematical framework remains exactly the same. Thus, as many spectral bands may be added as one wishes. The only limit is one of utility. Mueller (1976) suggests that, for open ocean waters, 4 to 5 spectral bands, properly chosen, may be sufficient to describe fully the variations in ocean color. Several more bands might be needed to describe completely the color variation of coastal waters, including polluted waters.

A second comment is that the assumptions made in formulating this description of variations in ocean color are simplifications. For instance, most multispectral satellite data cover rather large areas

TABLE 1. ANGULAR SEPARATION (IN DEGREES) BETWEEN PRIMARY EIGENVECTORS.

			IRON-ACID WASTE							SEDIMENT				CLOUDS				ICE
			24 FEB 76	19 JAN 76	21 OCT 75	19 AUG 75	17 NOV 75	15 MAR 74	AVERAGE	24 FEB 76 (NORTH)	24 FEB 76 (SOUTH)	19 JAN 76	AVERAGE	19 JAN 76	19 AUG 76	15 MAR 74	AVERAGE	19 JAN 76
			1	2	3	4	5	6	7	8	9	10	11	12	13	14	15	16
ACID	24 FEB 76	1	—															
	19 JAN 76	2	14.4	—														
	21 OCT 75	3	3.9	13.7	—													
	19 AUG 75	4	12.7	6.2	10.5	—												
	17 NOV 75	5	4.4	13.6	7.8	13.8	—											
	15 MAR 74	6	6.3	10.7	8.6	11.6	3.3	—										
	AVERAGE	7	8.5	11.1	8.6	10.3	8.8	7.9	—									
SEDI-MENT	24 FEB 76	8	36.1	22.9	33.9	23.7	36.4	33.5	31.5	—								
	24 FEB 76	9	37.9	24.8	35.7	25.4	38.3	35.4	33.3	2.0	—							
	19 JAN 76	10	34.2	22.6	31.4	21.8	35.2	32.7	30.1	6.1	6.5	—						
	AVERAGE	11	36.1	23.5	33.7	23.6	36.6	33.8	31.8	3.6	3.9	5.1	—					
CLOUDS	19 JAN 76	12	47.2	33.8	45.9	35.7	46.1	42.9	42.2	19.8	18.9	24.1	21.0	—				
	19 AUG 76	13	31.6	18.5	30.8	21.3	30.2	26.9	27.0	16.9	17.8	20.2	18.3	16.2	—			
	15 MAR 74	14	39.4	25.7	38.1	27.8	38.4	35.2	34.5	13.5	13.4	18.0	15.1	8.3	9.2	—		
	AVERAGE	15	39.8	26.7	38.7	28.8	38.7	35.5	35.0	16.9	16.9	20.9	18.3	10.5	10.8	7.2	—	
ICE	19 JAN 76 AVERAGE	16	42.6	28.6	41.1	30.6	41.9	38.7	37.6	11.2	10.5	16.5	13.0	9.4	14.3	5.9	10.4	—

over which the atmospheric conditions will often vary enough to introduce a lot of "noise" into the analysis. In such cases, the use of eigenvector analysis may be restricted to analysis of small areas. The analysis procedure was developed under a NASA grant and is described in detail in the final report (Klemas and Philpot, 1979).

For our present purposes we will limit ourselves to the angular separation of the eigenvectors as a measure of spectral separability. Table 1 shows the results of analyzing six different coastal Delaware Landsat scenes for sediment, ice, clouds, and an acid-iron industrial waste. There is some dispersion among vectors identifying each material resulting solely from the use of data acquired on different days. This dispersion amounts to ~6° for sediment, ~10° for the acid waste, and ~10° for clouds. The angular separation between different substances is always significantly higher; however, between acid and sediment it is about 35° while between acid and clouds it is about 40°.

To demonstrate what this means in terms of classification, two of these scenes were chosen in which there was some uncertainty as to what was cloud and what was acid. The eigenvector analysis was used to classify each pixel in both scenes as either acid, sediment, clouds, or clear water. The results are shown in Figures 6 and 7. In Figures 6a and 7a the clouds and acid are both plotted as dark points. The light areas correspond to clear water. (Less than twenty points out of tens of thousands were classified as sediment in both cases. These points were treated as clear water.) In Figures 6b and 7b only those pixels actually classified as acid-iron were plotted. The results are particularly striking in Figure 6b. The pattern that is seen in the course followed by the acid-iron barge while dumping. There is some noise in the background and there are some gaps in the pattern caused by clouds directly over the dump track, but generally the distinction is quite good. The results illustrated in Figure 7b are still good although much more noisy. The waste had been in the water for more than 6 hours as compared to a fresh dump in the earlier example. Because of dispersion and settling, the signal is not as clear, as is apparent in the relatively higher noise level. Still, it is clear that the acid was dumped in a straight line track on this day and that the other linear feature in the scene was a cloud.

Note that this is not a method for "seeing through" cloud cover, but only a method of distinguishing one target from another. The gaps in the pattern in Figure 6 represent areas that were covered by clouds, not real gaps in the dumping pattern. This method is similar in some ways to the chromaticity pattern approach to cloud detection described by Munday (1976) in which clouds and water types occupy distinct loci in the chromaticity diagrams. The two methods are comparable

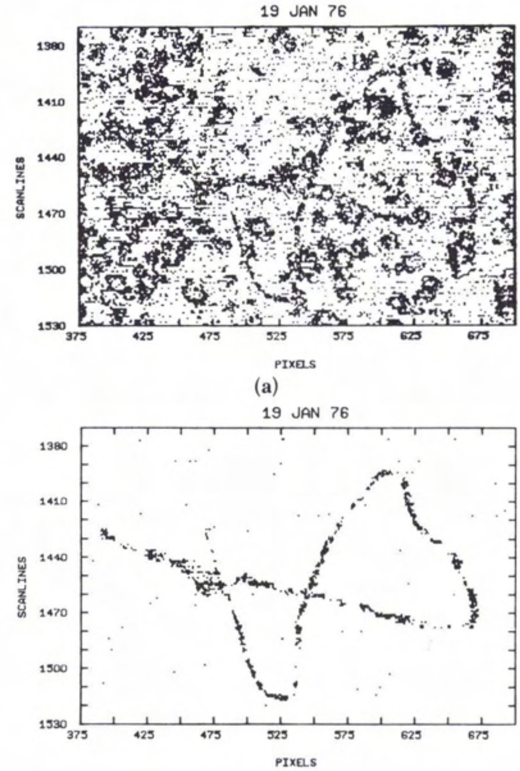

FIG. 6. (a) Original computer printout of iron-acid waste plume of 19 January 1976, against a cloud background. (b) Enhancement of the iron-acid waste plume of 19 January 1976, with cloud background removed.

in that both keep all the information available (in three bands, at least) and both can be interpreted geometrically. The chromaticity diagram, however, is restricted to a three-color (three-band) system while the eigenvector method is easily extended to any number of bands.

Preliminary results indicate that this approach can be extended with the Landsat data to include several other substances, and that considerably better results could be achieved using spectral channels more appropriate for analysis of water, such as those on the Coastal Zone Color Scanner (Hovis, 1977; Philpot, 1980).

Application of Current Drogues

A total of nine cruises were made to the acid-iron waste disposal site during the period from May 1975 to June 1976 to lauch radio-signal-emitting current drogues. Four of the cruises were made when a summer thermocline was present. The other five cruises were made during the winter months when isothermal conditions existed in this area. During each cruise three or four current drogues were deployed to measure currents at the

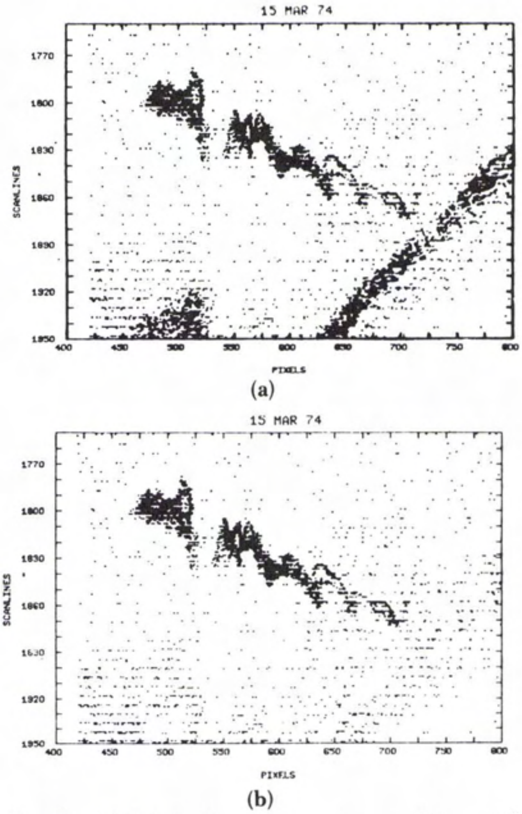

FIG. 7. (a) Original computer printout of iron-acid waste plume of 15 March 1974, against a cloud background. (b) Enhancement of the iron-acid waste plume of 15 March 1974, with a cloud background removed.

surface, mid-depth or above the thermocline, and below the thermocline. Also weather and sea conditions were noted during each cruise and a temperature profile was made to determine the presence and depth of the thermocline.

The drogues which are described by Klemas *et al.* (1977) radiate about 100 milliwatts of power in the 2- to 6-megahertz band. When using the sea surface as a ground plane and transmitting via ground wave, ranges in excess of 160 km have been obtained. Position finding was accomplished by triangulation from two radio direction-finding (DF) stations located on-shore near the water's edge. At an average distance of 65 km a standard deviation in bearing angle to a drogue of about 1 degree was obtained. To maintain this accuracy, each DF set had to be recalibrated on a moored drogue before each series of measurements. Best results were obtained for tracking ranges of about 15 to 100 km (Klemas *et al.*, 1978).

Discussion of Results

As shown in Table 2 and Figure 3, the maximum range of measurable wastes estimated by Falk (1974) as being about 18.5 km from the discharge point was in part substantiated by the satellite imagery, because only one out of 16 plumes was observed to be significantly beyond this range. This was also the only plume observed by the satellite as being 32 km from shore, with two others about 40 km from shore, and all remaining 13 plumes more than 48 km from shore. Waste plume drift speeds derived from Landsat imagery ranged from 0.46 km hr^{-1} (0.25 knot) to 2.74 km hr^{-1} (1.48 knots), with an average of 1.1 km hr^{-1} (0.59 knot).

TABLE 2. WASTE PLUME CHARACTERISTICS DERIVED FROM Landsat IMAGERY

	Date	Hours After Dump	Lateral Extent (km)	Plume Axis Orientation	Distance Between Centroids (km)	Drift Vector Orientation	Average Drift Velocity km hr^{-1}	(knots)
1)	10/10/72	9.63	18.5	155°	15.7	250°	1.63	(0.88)
2)	10/27/72	14.13	9.3	260°	7.4	225°	0.52	(0.28)
3)	01/25/73	3.05	9.3	120°	8.3	275°	2.74	(1.48)
4)	04/07/73	6.63	14.8	110°	5.6	280°	0.83	(0.45)
5)	05/13/73	0.00	1.9	105°	5.6	260°	0.00	(0.00)
6)	10/22/73	29.50	26.9	225°	22.2	195°	0.76	(0.41)
7)	10/23/73	53.60	25.9	200°	45.4	215°	0.85	(0.46)
8)	04/20/74	13.78	13.0	145°	13.0	215°	0.94	(0.51)
9)	05/26/74	24.33	13.9	145°	19.4	235°	0.89	(0.48)
10)	11/04/74	14.00	13.0	240°	6.5	110°	0.52	(0.28)
11)	08/19/75	0.00	13.9	120°	2.8	160°	0.00	(0.00)
12)	08/28/75	0.00	11.1	220°	2.8	270°	0.00	(0.00)
13)	10/21/75	6.58	14.8	250°	11.9	188°	1.80	(0.97)
14)	11/17/75	5.00	14.8	120°	3.7	160°	0.74	(0.40)
15)	01/19/76	3.00	12.0	245°	3.7	245°	1.24	(0.67)
16)	02/24/76	6.00	18.5	105°	7.4	135°	1.24	(0.67)
	AVERAGE		14.5		9.8		1.09	(0.59)

A total of 35 current drogues were released at the waste disposal site during the time period from May 1975 through June 1976. The drogues were successfully tracked from one to 13 days, with the average drift speeds of surface drogues ranged from 0.10 km hr^{-1} (0.05 knot) to 3.52 km hr^{-1} (1.9 knots), with a combined average of 0.85 km hr^{-1} of (0.46 knot). The near-bottom drogues moved at average speeds of 0.11 km hr^{-1} (0.06 knot) to 2.22 km hr^{-1} (1.2 knots), with a combined average of 0.67 km hr^{-1} (0.36 knot). However, since only several near-bottom drogues survived for more than two days, near-bottom results may not represent "typical" conditions.

Most of the current drogues, which were part of another study, were not released or being tracked during satellite overpasses. However, the average magnitudes of waste plume and drogue drift velocities are compatible with each other and with net current velocities measured by Falk (1974) and Myers (1974), including their maximum recorded net drift speed of 14 km d^{-1} (0.32 knot). Drogues were being released at the time of the 21 October 1975 pass of Landsat over an acid waste plume (Table 2). During the first six hours after dump the waste plume had drifted south (188° azimuth) at a velocity of 1.80 km hr^{-1} (0.97 knot). During the same period the near-surface drogue moved south-southeast (175° azimuth) at 1.96 km hr^{-1} (1.06 knots) and the 20-m depth drogue drifted to the south-southwest (190° azimuth) at 1.57 km hr^{-1} (0.85 knot). Since the waste plume disperses during the first few hours over intermediate depths, its drift direction and velocity lie between those of the two drogues. Twenty-four hours later the same plume was observed by aircraft at a distance of about 10.3 km and an azimuth direction of 166° from its location in the satellite image. The slowing of the plume drift velocity to 0.87 km hr^{-1} (0.47 knot) and change in direction indicates that, similar to the drogues, a north-easterly current component has been temporarily superimposed on the southward movement. The cause of this northeast current was most likely a steady 37 km hr^{-1} (20 knots) wind from the west which developed during that same period.

During the stratified warm months, more drogues tended to move in the north northeast direction while during the non-stratified winter months a southwest direction was preferred. These results do not conflict with previous studies which found that there was a mean flow to the southwest, with stratified surface waters moving in the northerly or north-westerly direction during the summer (Bumpus, 1965, 1969, 1973; Ketchum, 1953). Identical drogues released at equal depths generally followed similar paths. However, drogues released at different depths frequently traveled along different paths and at different speeds, indicating the presence of current shear.

Most rapid movement of the drogues at all depths occurred during a severe northeaster storm with drogue speeds in excess of 3.33 km hr^{-1} (1.8 knots) being attained. Thus, the circulation process at the waste dump site appears to be highly storm-dominated with an increase of water transport occurring during storms, particularly northeasters. This conclusion is in agreement with results obtained by other investigators in the Middle Atlantic Bight (Beardsley *et al.*, 1974).

As shown in Figure 8, a distinct summer thermocline was observed from June through August 1975 at depths ranging from 13 m to 24 m. In 1976, the first observation of a thermocline again occurred in June. The strongest thermocline was observed on 19 August 1975, having a change of temperature from 23° to 8°C between depths of 13 m and 20 m, respectively. In comparison, Myers (1974) observed the formation of a thermocline at the same site during April 1973 at depths between 18 m and 23 m. Ocean stratification conditions influence waste dispersion. The wastes do not reach the ocean bottom when a thermocline is present. They are distributed from top to bottom when the ocean is isothermal (Falk, 1974).

The spatial and temporal resolution of the satellite imagery was not sufficient to provide precise data on waste plume dispersion. However, a visual estimate of plume width was obtained from satellite imagery and plotted as a function of time after dump in Figure 4. As shown in Figure 4, the plume width spreading rates range from about 0.5 cm sec^{-1} to about 6 cm sec^{-1}. During calm seas the plume width increased at an average rate of about 1.5 cm sec^{-1}, while during wind-dominated, rough sea conditions, spreading rates in excess of 4 cm sec^{-1} were attained. On days when wind

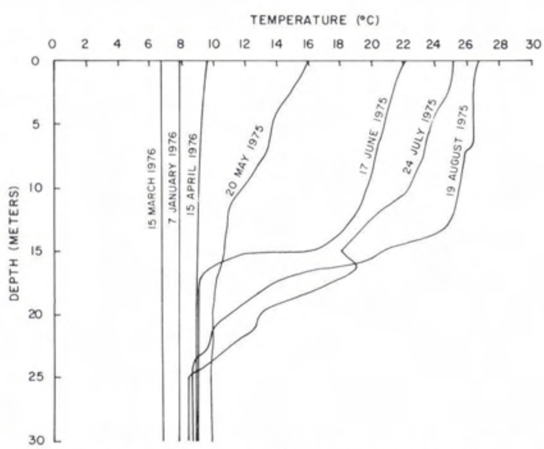

FIG. 8. Temperature profiles obtained with an expendable bathythermograph showing water stratification and formation of a thermocline during summer months.

velocities exceeded 15 km hr^{-1}, rapid formation of regular patches (Langmuir cells) was evident in that section of the plume which was not parallel to the wind direction.

Conclusions

Satellites such as Landsat offer an effective means of assessing the drift and dispersion of industrial wastes dumped on the continental shelf. This is particularly true for the acid wastes disposal about 64 km off the Delaware coast since these wastes form a sparse but optically persistent ferric floc which can be observed by Landsat's multispectral scanner band 4 up to two days after dump.

Most of the 16 waste plumes imaged by Landsat were found to be drifting at average rates of 0.59 km hr^{-1} (0.32 knot) to 3.39 km hr^{-1} (1.83 knots) into the southwest quadrant. The plumes seemed to remain above the thermocline, which was observed to form from June through August at a depth ranging from 13 m to 24 m. During the remainder of the year, the ocean at the test site was not stratified, permitting wastes to mix throughout the water column to the bottom (Falk, 1974).

The magnitudes of plume drift velocities were compatible with the drift velocities of current drogues released over a 12-month period at the surface, at mid-depth, and near the bottom. However, during the stratified warm months, more drogues tended to move in the north-northeast direction, while during the non-stratified winter months a southwest direction was preferred. Drogues released at different depths frequently traveled along different paths and at different speeds, indicating the presence of current shear.

Rapid movement toward shore occurs primarily during storms, particularly northeasters. During such storms, however, the plume is rapidly dispersed and diluted. The plume width was observed to increase at a rate of about 1.5 cm sec^{-1} during calm sea conditions, yet attain spread rates in excess of 4 cm sec^{-1} on days when winds reached speeds of 24 km hr^{-1} (13 knots) to 38 km hr^{-1} (21 knots). These results are in agreement with Falk's (1974) estimate of plume dilution shown in Figure 9, which indicates that, by the time a waste plume moves 37 km from the dump site, dilution is at least one million to one.

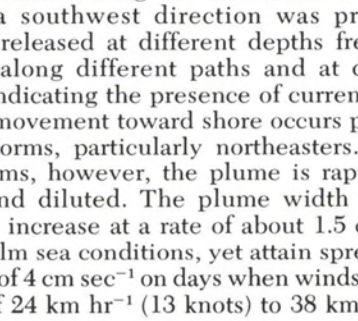

FIG. 9. Estimated dilution of waste plume as a function of distance from dump site at the time of satellite overpass (Falk, 1974).

Acknowledgments

The research projects described in this article were partly funded through NASA, Contract Number NAS5-20983; and a contract from E. I. DuPont de Nemours and Company.

References

Apel, J. R., R. V. Charnell, and R. J. Blackwell, 1974. Ocean internal waves off the North American and African coasts from ERTS-1. *Proceedings, Ninth International Symposium on Remote Sensing of Environment*, Ann Arbor, Michigan, Vol. 2, pp. 1345-1351.

Beardsley, R. C., and B. Butman, 1974. Circulation on New England Continental Shelves: Response to Strong Winter Storms. *Geo-Physical Research Letters*, Vol. 1, p. 181.

Boicourt, W. C., and P. W. Hacker, 1976. Circulation on the Atlantic Continental Shelf of the United States, Cape May to Cape Hatteras. *Memoires Societe Royale des Sciences de Liege*, 6th Series, Vol. 10, p. 187.

Bumpus, D. F., 1965. Residual Drift Along the Bottom of the Continental Shelf in the Middle Atlantic Bight Area. *Limnol. Oceanography*, Vol. 10, p. 50.

———, 1969. Reversals in the Surface Drift in the Middle Atlantic Bight Area. *Deep-Sea Resources*, pp. 16-17.

———, 1973. Physical Oceanography. In *Coastal and Offshore Environmental Inventory, Cape Hatteras to Nantucket Shoals*. Marine Publication Series No. 2, University of Rhode Island, Kingston, Rhode Island.

Bumpus, D. F., and L. M. Lauzier, 1965. *Surface Circulation on the Continental Shelf off Eastern North America Between Newfoundland and Florida.* American Geographical Society, New York, Folio 7, Serial Atlas of the Marine Environment.

Fader, S. W., 1972. Barging Industrial Liquid Wastes to the Sea. *Journal Water Pollution Control Federation*, Vol. 44, p. 314.

Falk, L. L., 1974. *Waste Dispersion Characteristics and Effects in an Oceanic Environment.* Report prepared for U.S. Environmental Protection Agency, Program No. 12020 EAW.

Gordon, H. R., O. B. Brown, and J. Jacobs, 1975. Computer Relationships Between the Inherent and Apparent Optical Properties of a Flat Homogeneous Ocean. *Applied Optics* 14, pp. 417-427.

Gordon, H. R., 1978. Remote Sensing of Optical Properties in Continuously Stratified Waters. *Applied Optics* 17(12), pp. 1893-1897.

Hovis, W. A., Jr., 1977. Remote Sensing of Water Pollution. *Proceedings, 11th International Symposium on Remote Sensing of Environment*, Ann Arbor, Michigan, pp. 361-362.

Johnson, R. W., and C. W. Ohlhorst, 1980. Application of Remote Sensing to Monitoring and Studying Dispersion in Ocean Dumping. *Proceedings of 1st International Ocean Dumping Symposium*, Kingston, Rhode Island. (In Press)

Ketchum, H., 1953. *Preliminary Evaluation of the Coastal Water Off Delaware Bay for the Disposal of Industrial Wastes*. Unpublished Manuscript, Reference No. 55-31, Woods Hole Oceanographic Institution, Woods Hole, Massachusetts.

Klemas, V., G. R. Davis, and R. D. Henry, 1977a. Satellite and Studies of Ocean-Disposed Waste Drift. *Journal Water Pollution Control Federation*, Vol. 49(5), pp. 757-763.

Klemas, V., G. R. Davis, J. Lackie, W. Whale, and G. Tornatore, 1977b. Satellite, Aircraft and Drogue Studies of Coastal Currents and Pollutants. *IEEE Transactions on Geoscience Electronics*, Vol. 2(2), pp. 119-126.

Klemas, V., and W. Philpot, 1979. *Detection of Ocean Waste in the New York Bight*. Final Report. NASA Grant NSG 1398, Prepared for NASA Langley Research Center, 15 March 1979.

Morrison, D. F., 1976. *Multivariate Statistical Methods*, McGraw-Hill, New York, 2nd Edition.

Mueller, J. L., 1976. Ocean Color Spectra Measured off the Oregon Coast: Characteristic Vectors. *Applied Optics* 15, pp. 395-402.

Munday, J. C., 1974. Lake Ontario Water Mass Delineation. *Proceedings, 9th International Symposium on Remote Sensing of Environment*, pp. 1355-1368.

Myers, T. D., 1974. An Observation of Rapid Thermocline Formation in the Middle-Atlantic Bight. *Estuarine and Coastal Marine Science*, Vol. 2, p. 74.

Ohlhorst, C. W., and G. S. Bahn, 1979. Mapping of Particulate Iron in an Ocean Dump. *Photogrammetric Engineering and Remote Sensing*, Vol. 45(8), pp. 1117-1122.

Peschiera, L., and F. Freiherr II, 1968. Disposal of Titaniumn Pigment Process Wastes. *Journal Water Pollution Control Federation*, Vol. 41, p. 127.

Plass, G. N., P. J. Humphreys, and G. W. Katawar, 1978. Color of the Ocean. *Applied Optics*, Vol. 17(9), pp. 1432-1446.

Polcyn, F. C., and I. J. Sattinger, 1979. *Marine Ecosystem Analysis Program: A Summary of Remote Sensing Investigations in the New York Bight*. ERIM Report 131200-1-F, Ann Arbor, Michigan.

Simmonds, J. L., 1963. Application of Characteristic Vector Analysis to Photographic and Optical Response Data. *Journal Optical Society of America*, Vol. 55, pp. 968-974.

U.S. Environmental Protection Agency, 1975. Interim Ocean Dumping Permit DE006, Issued to E. I. DuPont de Nemours and Company, Inc. by EPA Region III, Philadelphia, Pennsylvania.

(Received 21 March 1980; revised and accepted 23 September 1980)

38th Photogrammetric Week

Stuttgart, Federal Republic of Germany
5–10 October 1981

Cosponsored by the Institute for Photogrammetry of Stuttgart University and the Division for Geodesy and Photogrammetry of Carl Zeiss, Oberkochen, the 38th Photogrammetric Week will be under the scientific direction of Prof. F. Ackermann, Stuttgart, and Prof. H.-K. Meier, Oberkochen. The lecturers, from Germany and abroad, will put special emphasis on

- Aerial Photography
- Digital Terrain Models

The meeting will open with the award of the Carl Pulfrich prize 1981 and reports of the organizers, and will conclude with individual lectures on aerotriangulation.

Experienced technical interpreters will give simultaneous translations of the mostly German lectures into English, French, and Spanish. The lectures will be unabridged; sufficient time has been allowed for discussions.

The program is rounded off with demonstrations and practical exercises on three afternoons.

For further information please write to

Universität Stuttgart
Institut für Photogrammetrie
Postfach 560, Keplerstrasse 11
D-7000 Stuttgart 1, Fed. Rep. of Germany